

## MIT Open Access Articles

*Dual recognition of phosphoserine and phosphotyrosine in histone variant H2A.X by DNA damage response protein MCPH1*

The MIT Faculty has made this article openly available. **Please share** how this access benefits you. Your story matters.

**Citation:** Singh, N. et al. "Dual Recognition of Phosphoserine and Phosphotyrosine in Histone Variant H2A.X by DNA Damage Response Protein MCPH1." Proceedings of the National Academy of Sciences 109.36 (2012): 14381–14386. CrossRef. Web.

**As Published:** <http://dx.doi.org/10.1073/pnas.1212366109>

**Publisher:** National Academy of Sciences (U.S.)

**Persistent URL:** <http://hdl.handle.net/1721.1/78280>

**Version:** Final published version: final published article, as it appeared in a journal, conference proceedings, or other formally published context

**Terms of Use:** Article is made available in accordance with the publisher's policy and may be subject to US copyright law. Please refer to the publisher's site for terms of use.



# Dual recognition of phosphoserine and phosphotyrosine in histone variant H2A.X by DNA damage response protein MCPH1

Namit Singh<sup>a,1</sup>, Harihar Basnet<sup>b,1</sup>, Timothy D. Wiltshire<sup>c</sup>, Duaa H. Mohammad<sup>d,e</sup>, James R. Thompson<sup>f</sup>, Annie Héroux<sup>g</sup>, Maria Victoria Botuyan<sup>a</sup>, Michael B. Yaffe<sup>d,e</sup>, Fergus J. Couch<sup>c</sup>, Michael G. Rosenfeld<sup>b,2</sup>, and Georges Mer<sup>a,2</sup>

Departments of <sup>a</sup>Biochemistry and Molecular Biology, <sup>c</sup>Laboratory Medicine and Pathology, and <sup>f</sup>Physiology and Biomedical Engineering, Mayo Clinic, Rochester, MN 55905; <sup>b</sup>Howard Hughes Medical Institute and Graduate Program in Biomedical Sciences, University of California at San Diego, School of Medicine, La Jolla, CA 92093; Departments of <sup>d</sup>Biology and <sup>e</sup>Biological Engineering, Massachusetts Institute of Technology, Cambridge, MA 02139; and <sup>g</sup>Biology Department, Brookhaven National Laboratory, Upton, NY 11973

Contributed by Michael G. Rosenfeld, July 22, 2012 (sent for review April 19, 2012)

**Tyr142, the C-terminal amino acid of histone variant H2A.X is phosphorylated by WSTF (Williams-Beuren syndrome transcription factor), a component of the WICH complex (WSTF-ISWI chromatin-remodeling complex), under basal conditions in the cell. In response to DNA double-strand breaks (DSBs), H2A.X is instantaneously phosphorylated at Ser139 by the kinases ATM and ATR and is progressively dephosphorylated at Tyr142 by the Eya1 and Eya3 tyrosine phosphatases, resulting in a temporal switch from a postulated diphosphorylated (pSer139, pTyr142) to monophosphorylated (pSer139) H2A.X state. How mediator proteins interpret these two signals remains a question of fundamental interest. We provide structural, biochemical, and cellular evidence that Microcephalin (MCPH1), an early DNA damage response protein, can read both modifications via its tandem BRCA1 C-terminal (BRCT) domains, thereby emerging as a versatile sensor of H2A.X phosphorylation marks. We show that MCPH1 recruitment to sites of DNA damage is linked to both states of H2A.X.**

Preserving genomic integrity is vital to the fitness of an organism. Damage to DNA emanating from endogenous and exogenous insults can trigger signaling cascades relayed by posttranslational modifications culminating in the activation of the cell cycle checkpoint and initiation of repair. One of the key initiating events in this process is the phosphorylation at serine 139 (pSer139) of histone H2A.X, a chromatin-bound histone variant (1, 2). Phosphorylated H2A.X ( $\gamma$ H2A.X) serves as a platform for the recruitment of downstream mediator proteins as well as chromatin modifying proteins to the affected site (3–5). Recent studies have added a new dimension to the recognition of  $\gamma$ H2A.X with the identification of a new phosphorylation site in H2A.X, Tyr142. In response to DNA damage, Tyr142 was found to transition from a phosphorylated (pTyr142) to a non-phosphorylated state in an Eya1/3 phosphatase-dependent manner (6–8). Whereas the dephosphorylation of pTyr142 is gradual, the phosphorylation of Ser139 is prompt, and the overlap in the two processes is thought to give rise to the doubly phosphorylated (pSer139, pTyr142) H2A.X state (di- $\gamma$ H2A.X) following genotoxic insult (6, 7). The existence of di- $\gamma$ H2A.X and proteins that recognize this state remain open questions in the field.

The protein MDC1 (mediator of DNA damage checkpoint 1) has emerged as an interacting partner of  $\gamma$ H2A.X. MDC1 was found to directly sense pSer139 and to mobilize the downstream response by virtue of its tandem BRCA1 C-terminal (BRCT) domains (4, 5). An important question therefore is how MDC1, an established  $\gamma$ H2A.X binder, responds to the presence of diphosphorylated H2A.X. Interestingly, several groups have independently found that MDC1 does not interact with di- $\gamma$ H2A.X (6, 7, 9). Indeed, efforts to identify binding partners of a di- $\gamma$ H2A.X peptide were redirected at well-established pTyr-binding SH2/PTB domains and led to the second PTB domain of Fe65 as a possible target (7). Is this inability to bind Tyr142-phosphorylated

H2A.X reflective of the inherent limitations of tandem BRCT domains, previously identified as pSer or pThr binding domains, to recognize the pTyr state?

*Microcephalin (MCPH1)*, the first gene identified as causative for primary autosomal microcephaly (10), has been linked to various cellular processes including the DNA damage checkpoint, DNA repair by homologous recombination, and DNA transcription (11–15). Previous studies have established that MCPH1 is an early responder in the DNA damage response (DDR) and regulates the recruitment of several downstream mediator proteins, a characteristic shared with MDC1. Similarities between MCPH1 and MDC1 are inescapable. Both proteins include tandem BRCT domains at their C terminus that are necessary for irradiation-induced foci (IRIF) formation in an H2A.X pSer139 phosphorylation-dependent manner (16, 17). MCPH1 and MDC1 can bind a peptide that encompasses phosphorylated Ser139 (16, 18) and in vivo mutation of this residue results in loss of IRIF (16). Because MCPH1 IRIF formation necessitates  $\gamma$ H2A.X, presumably because of direct interaction with  $\gamma$ H2A.X, we asked whether MCPH1 could also interact with di- $\gamma$ H2A.X.

The discovery that H2A.X Tyr142 can be phosphorylated has raised several interesting points. First, whereas the di- $\gamma$ H2A.X species has been suggested, a deeper characterization of its kinetics and role in DNA damage remains to be attempted. Second, it remains to be determined whether a relationship exists between di- $\gamma$ H2A.X and  $\gamma$ H2A.X. Third, it is not known whether MCPH1, a previously described  $\gamma$ H2A.X interactor, can also recognize di- $\gamma$ H2A.X. Here, via the generation of an antibody that selectively recognizes a di- $\gamma$ H2A.X peptide (di-pH2A.X), we demonstrate the existence of di- $\gamma$ H2A.X and monitor its dynamics following DNA damage. Furthermore, we show that there exists a direct relationship between pTyr142 and pSer139, whereby the former affects the latter. Most importantly, our work identifies MCPH1 as a BRCT protein that directly interacts with di-pH2A.X and explains the structural basis for this recognition. Hitherto, BRCT domains were thought to function within the realm of pSer or pThr recognition (19–21).

Author contributions: N.S., H.B., M.G.R., and G.M. designed research; N.S., H.B., T.D.W., D.H.M., J.R.T., A.H., M.V.B., M.B.Y., F.J.C., and G.M. performed research; N.S., H.B., M.G.R., and G.M. analyzed data; and N.S., H.B., and G.M. wrote the paper.

The authors declare no conflict of interest.

Freely available online through the PNAS open access option.

Data deposition: The atomic coordinates for the structures of MCPH1-pH2A.X and MCPH1-di-pH2A.X complexes have been deposited in the Protein Data Bank, [www.pdb.org](http://www.pdb.org) (PDB ID codes 3S2M and 3U3Z).

<sup>1</sup>N.S. and H.B. contributed equally to this work.

<sup>2</sup>To whom correspondence may be addressed. E-mail: mer.georges@mayo.edu or mrosenfeld@ucsd.edu.

This article contains supporting information online at [www.pnas.org/lookup/suppl/doi:10.1073/pnas.1212366109/-DCSupplemental](http://www.pnas.org/lookup/suppl/doi:10.1073/pnas.1212366109/-DCSupplemental).

## Results

To directly examine the role of di- $\gamma$ H2A.X in the DDR, we developed an antibody specific to di- $\gamma$ H2A.X. This antibody preferentially recognizes di- $\gamma$ H2A.X among the four possible posttranslational states of H2A.X and could be completely blocked with a di- $\gamma$ H2A.X peptide but not with the corresponding nonphosphorylated peptide (Fig. S1). Using this reagent, we tracked the kinetics of di- $\gamma$ H2A.X in *H2a.x*<sup>-/-</sup> mouse embryonic fibroblasts (MEFs) reconstituted with wild-type H2A.X and determined that di- $\gamma$ H2A.X levels peak 1 h postirradiation and decline rapidly thereafter (Fig. 1A). Because immunofluorescence allows visualization of  $\gamma$ H2A.X as distinct nuclear foci after exposure to ionizing radiation (Fig. S2), we then asked whether di- $\gamma$ H2A.X behaves similarly. We observed that di- $\gamma$ H2A.X, much like  $\gamma$ H2A.X, forms IRIF following DNA damage (Fig. 1C). Next, using *H2a.x*<sup>-/-</sup> MEFs stably reconstituted with either wild-type or Y142F mutant H2A.X, we monitored the kinetics of  $\gamma$ H2A.X in both cell lines (Fig. 1A and B). Interestingly, the Y142F mutant showed an increase in  $\gamma$ H2A.X until 30 min after irradiation, and then was rapidly reduced to undetectable levels by 1 h postirradiation, whereas the wild-type H2A.X reconstituted cells sustained a high level of  $\gamma$ H2A.X even at 10 h postirradiation (Fig. 1A and B). This result implies that Tyr142 phosphorylation in H2A.X is necessary for retaining  $\gamma$ H2A.X after DNA damage. A similar defect in the kinetics of  $\gamma$ H2A.X has been shown in cells where expression of the Tyr142-specific kinase WSTF (Williams-Beuren syndrome transcription factor) was knocked down (6). The defect in  $\gamma$ H2A.X kinetics

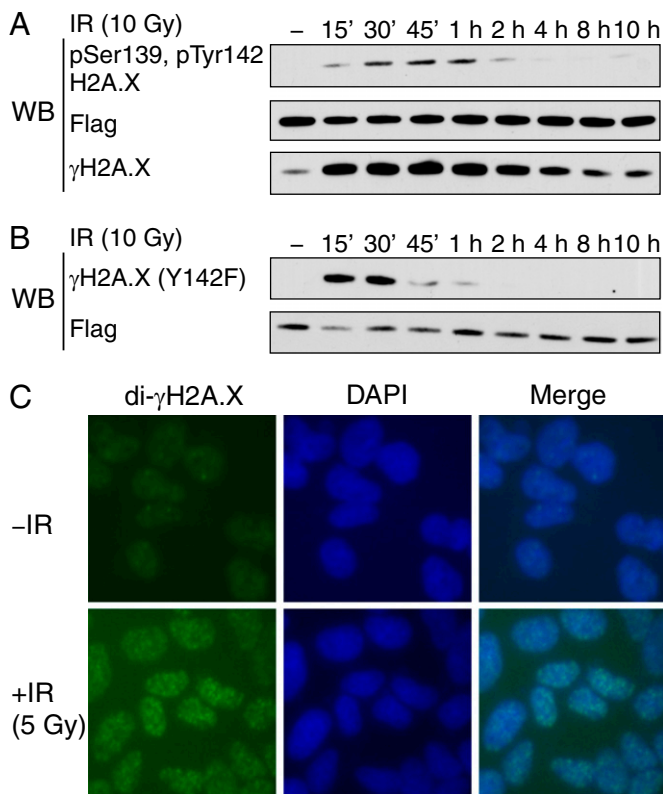


**Fig. 1.** Diphosphorylated H2A.X is critical in mediating the DNA damage response. (A) *H2a.x*<sup>-/-</sup> MEFs were stably reconstituted with Flag-SBP-tagged wild-type (WT) H2A.X. Cells were irradiated for 1 h at 10 Gy and the whole cell lysate was immunoblotted with the indicated antibodies. (B) Same as A but the MEFs were transfected with the Y142F H2A.X mutant. (C) Di- $\gamma$ H2A.X foci were visualized in 293T cells by immunofluorescence staining before and after exposure to ionizing radiation (IR) for 1 h at 5 Gy.

impairs the formation of MDC1 and phosphorylated ATM foci postirradiation (6). Taken together, these results validate the postulated di- $\gamma$ H2A.X state, confirm the interplay between di- $\gamma$ H2A.X and  $\gamma$ H2A.X, and suggest that di- $\gamma$ H2A.X can critically influence the DDR pathway.

MCPH1 is a DDR protein that is recruited to the sites of DNA damage within minutes in a  $\gamma$ H2A.X-dependent fashion and this recruitment necessitates MCPH1 C-terminal tandem BRCT domains (11, 16, 17). Unlike many other repair factors, MCPH1 relocalization to DNA damage sites occurs even in the absence of MDC1 (16). We investigated whether the tandem BRCT domains of MCPH1 directly recognize  $\gamma$ H2A.X and di- $\gamma$ H2A.X. Using a phosphoserine-containing peptide library screen, we determined that the BRCT domains optimally bind the motif pSXXY where pS is the phosphoserine, X represents any amino acid, and position pS+3 is a tyrosine (Y), with a strong requirement for a free C-terminal carboxylate group (Fig. 2A). Histone  $\gamma$ H2A.X, which exhibits the optimal motif pSQEY, Y being the C-terminal residue of the protein, may represent a preferred binding target. This was validated using pull-down assays that confirmed an interaction between full-length MCPH1 and a  $\gamma$ H2A.X peptide that could be disrupted by single point mutations in MCPH1 (see below). Using isothermal titration calorimetry (ITC), we also determined that a Ser139-phosphorylated tetrapeptide corresponding to the C-terminal end of human H2A.X (pH2A.X, residues 139–142) binds the tandem BRCT domains of human MCPH1 with a dissociation constant ( $K_d$ ) of  $0.7 \pm 0.1 \mu\text{M}$ , whereas the peptide devoid of the phosphate group showed no interaction (Fig. 2B and Fig. S3).

Whereas MDC1 can directly bind  $\gamma$ H2A.X through its tandem BRCT domains, it fails to engage the di- $\gamma$ H2A.X state (6, 7, 9). We found that, unlike MDC1, MCPH1 could bind a diphosphorylated (pSer139, pTyr142) H2A.X tetrapeptide (di-pH2A.X, residues 139–142) with a  $K_d$  of  $4.4 \pm 0.3 \mu\text{M}$  (Fig. 2B). Furthermore, we observed partial and near complete colocalization of MCPH1 with di- $\gamma$ H2A.X and with  $\gamma$ H2A.X, respectively, consistent with their in vitro affinities (see below). Whereas tandem BRCT domains have been previously identified as pSer binding modules (19, 20), MCPH1 represents the singular instance of a tandem BRCT repeat that can interact with both a singly and a doubly phosphorylated motif accompanied by an inherent selectivity for one of the states.

To gain a deeper understanding of these interactions, we determined the structures of MCPH1 tandem BRCT domains (BRCT2–BRCT3) in complex with a pH2A.X decapeptide (MCPH1- $\gamma$ H2A.X) and di- $\gamma$ H2A.X tetrapeptide (MCPH1-di- $\gamma$ H2A.X) to 2.6-Å and 1.5-Å resolution, respectively (Fig. 3A and B and Table 1 and Figs. S4 and S5). Whereas  $\gamma$ H2A.X peptides adopt similar conformations when bound to either MCPH1 or MDC1 (Fig. 3C), a reorientation of di-pH2A.X Gln140 side chain is necessary for binding to MCPH1 (Fig. 3D). In fact, the rigid conformation of Gln140 was held partly responsible for the inability of MDC1 to interact with di-pH2A.X (9).

In the MCPH1- $\gamma$ H2A.X and MCPH1-di-pH2A.X structures, the phosphate of pSer139 is recognized via direct hydrogen bonding to MCPH1 Thr653, Ser654, and Asn696 (Fig. 3B and Fig. S5). Additionally, the higher resolution MCPH1-di-pH2A.X structure shows a network of water-mediated interactions involving the phosphate of pSer139 and the backbone carbonyl groups of Met652, Met655, and Pro677 as well as the backbone amide atoms of Asn696 (Fig. 3B). Thr653 resides in a position structurally identical to Thr1898 in MDC1 and Ser1655 in BRCA1 and binds the phosphate analogously (Fig. S6). Mutation of Thr653 to Ala dramatically reduced binding of the MCPH1 BRCT domains to the pSXXX C-terminal peptide library (Fig. 2A), whereas mutation of MCPH1 Asn696 to an aspartate resulted in greater than 500-fold reduction in affinity (Fig. S3). Noticeably, in MDC1 (4) and BRCA1 (22–25), and in



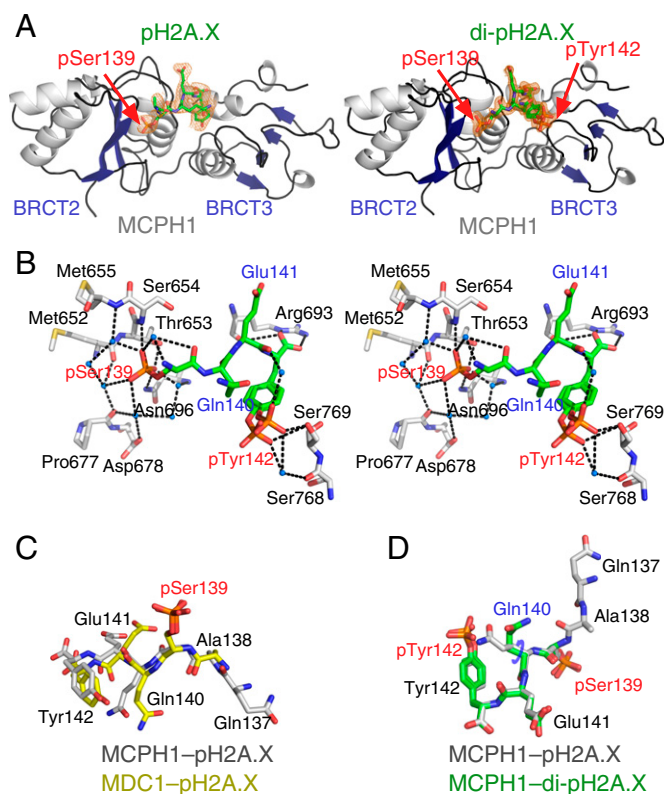


**Fig. 3.** Three dimensional structures of MCPH1 tandem BRCT domains in complex with pH2A.X and di-pH2A.X phosphopeptides. (A) Ribbon diagrams of the structures of MCPH1 C-terminal tandem BRCT domains (BRCT2 and BRCT3; residues 640–835) in complex with (Left) a pH2A.X decapeptide (residues 133–142) and (Right) a di-pH2A.X tetrapeptide (residues 139–142). The  $2F_o - F_c$  omit electron density maps of the peptides are shown contoured at  $1\sigma$  level (orange mesh). Note the two conformations of pTyr142 in the di-pH2A.X complex. (B) Stereographic representation of key residues of MCPH1 interacting with the di-pH2A.X peptide. Hydrogen bonds and water molecules are depicted as black dashes and blue spheres, respectively. (C) Overlay of a pH2A.X hexapeptide from the MCPH1-pH2A.X structure (gray) with a pentapeptide from the MDC1-pH2A.X structure (yellow). (D) Overlay of a pH2A.X hexapeptide from the MCPH1-pH2A.X structure (gray) and di-pH2A.X tetrapeptide from the MCPH1-di-pH2A.X structure (green). Note the different orientations of Gln140 side chains corresponding to a  $\chi_1$  angle change of  $\sim 86^\circ$ .

the tyrosine phosphate and Pro2009 in MDC1 specificity loop, or alternately, pTyr142 and the di-pH2A.X Gln140 side chain. However, we observed that in the MCPH1-di-pH2A.X complex this barrier is overcome by an altered conformation of di-pH2A.X that permits accommodation of the phosphotyrosine. This conformational change now results in the side chain of Gln140 pointing away from pTyr142 (Fig. 3D). Furthermore, the proline residue (Pro770), also present in the specificity loop of MCPH1 (Fig. S7A), does not hamper binding to di-pH2A.X. Because in MDC1 a glutamine (Gln2008) resides at a position equivalent to MCPH1 Ser769 that forms a hydrogen bond with the phosphate of pTyr142 in di-pH2A.X (Fig. S7A), we asked whether the Q2008S mutation in MDC1 would allow it to bind di-pH2A.X. This mutation, however, is insufficient to change its binding proclivity with respect to di-pH2A.X. MDC1 Q2008S retains tight binding to pH2A.X ( $K_d = 0.4 \pm 0.1 \mu\text{M}$ ) but, like the wild-type protein, does not bind di-pH2A.X ( $K_d > 200 \mu\text{M}$ ) (Fig. 2B). In contrast to MDC1, MCPH1 presents a more favorable electropositive surface in BRCT3 for the phosphotyrosine, possibly providing a permissive environment for binding (Fig. S7B). This

could explain why a single amino acid mutation is insufficient to convert MDC1 to an MCPH1-like state.

## Discussion

DNA damage initiates a complex cascade of chromatin modification, signaling, and repair events that are just beginning to be understood. Although there exist dedicated proteins attending to each of these processes, other proteins have a broader coordinating role in these pathways. The protein Microcephalin or MCPH1 is a case in point. MCPH1 is implicated in chromatin remodeling by virtue of its interaction with the SWI/SNF complex (15), in signaling programs via its association with Chk1 among other proteins (11, 29–32), and aids the DNA repair process by interacting with BRCA2 (33) and Condensin II (34, 35). Because of its involvement in multiple processes that converge to maintain genomic integrity, MCPH1 has been termed a “guardian of the genome” (13). Indeed, ablation of MCPH1 resulted in a menagerie of chromosomal defects that includes changes in both the nature and number of chromosomes, highlighting its importance in regulating genomic stability (12, 13). Furthermore, diminished DNA copy numbers as well as reduced MCPH1 mRNA and protein expression levels have been noted in several breast and ovarian cell lines and in ovarian cancer tissues, suggesting that MCPH1 is a putative tumor suppressor (12). Whereas considerable progress has been made regarding the biology of MCPH1, a central unanswered question is: how is this key regulator of genomic stability recruited to sites of DNA damage?

To probe MCPH1 recruitment to sites of DNA damage, its IRIF were visualized in cells devoid of various sensor and mediator proteins. MCPH1 foci were found to depend on  $\gamma\text{H2A.X}$  but were independent of ATM, MDC1, or NBS1 (16). Interestingly, whereas the down-regulation of MCPH1 resulted in several proximal as well as distal DDR proteins to be absent from the sites

**Table 1.** Data collection and refinement statistics

	MCPH1-pH2A.X	MCPH1-di-pH2A.X
Data collection		
Space group	$P1$	$P2_1$
Cell dimensions		
<i>a</i> , <i>b</i> , and <i>c</i> , Å	67.81, 82.23, and 104.42	37.69, 46.54, and 55.78
$\alpha$ , $\beta$ , and $\gamma$ °	72.10, 87.87, and 80.94	90.00, 97.07, and 90.00
Resolution (Å)	50.0–2.63 (2.74–2.63)*	50.0–1.50 (1.55–1.50)
$R_{\text{merge}}$	0.064 (0.471)	0.062 (0.437)
$I/\sigma I$	13.57 (2.70)	25.7 (2.3)
Completeness (%)	90.2 (97.8)	96.7 (80.1)
Redundancy	2.6 (2.6)	3.0 (2.6)
Refinement		
Resolution (Å)	50.0–2.63 (2.89–2.63)	23.79–1.50 (1.65–1.50)
No. reflections	56,418 (14,911)	29,928 (7,036)
$R_{\text{work}}/R_{\text{free}}$	20.1/25.2	12.9/17.1
No. atoms	14,108	2,063
Protein	13,294	1,720
Ligand/ion	422	54
Water	392	289
<i>B</i> factors		
Protein	66.4	20.9
Ligand/ion	56.3	24.9
Water	47.4	34.5
R.m.s. deviations		
Bond lengths, Å	0.009	0.005
Bond angles, °	1.05	1.071
Ramachandran plot		
Favored regions, %	98.0	99.0
Allowed regions, %	1.8	1.0

Each dataset was collected on a single crystal.

\*Values in parentheses are for highest-resolution shell.

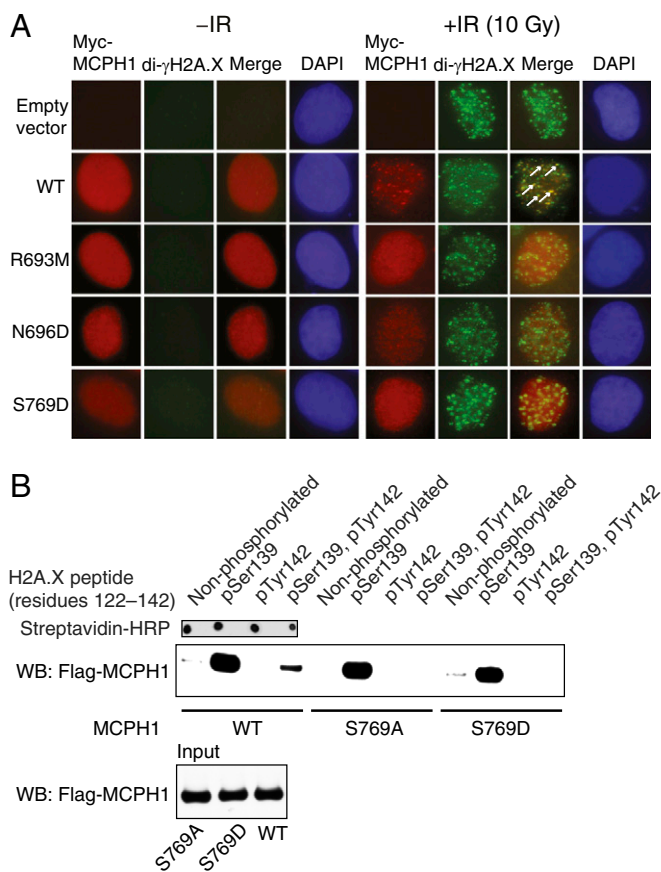


**Fig. 4.** Probing the MCPH1–di- $\gamma$ H2A.X interaction in cells. (A) U2OS cells were transfected with Myc-tagged wild-type (WT) or mutant MCPH1 and cells were coimmunostained with anti-Myc and anti- $\gamma$ H2A.X antibodies before and after exposure to 10 Gy of ionizing radiation (IR) for 1 h. Note that MCPH1 foci are almost completely colocalized with  $\gamma$ H2A.X foci (Fig. S2), whereas they are partially colocalized with di- $\gamma$ H2A.X foci, some of which are highlighted with white arrows. (B) 293T cells were transfected with Flag-tagged wild-type (WT) or indicated MCPH1 mutants, and nuclear extracts from the irradiated cells were incubated with a synthetic biotinylated H2A.X peptide (unmodified or phosphorylated as indicated) affixed to streptavidin-coated magnetic beads. Resulting pull-down products were analyzed by Western blot (WB) using an anti-Flag antibody.

of DNA damage including ATM, ATR, and Rad51, the formation of  $\gamma$ H2A.X foci remained unaffected (12). This suggests that MCPH1 recruitment is  $\gamma$ H2A.X-dependent and that MCPH1 does not regulate  $\gamma$ H2A.X foci formation.

Histone variant H2A.X is considered to occupy a sentinel position in the DDR, serving as a critical intermediary in relaying information pertaining to double-strand breaks (DSBs) to the outside environment. To understand how MCPH1 is mobilized to DSBs, we began investigating the interaction of the C-terminal end of MCPH1, previously deemed important for this anchoring process, with the different H2A.X states. Because chronologically pTyr142-containing H2A.X is present in the absence of DNA damage, we explored and found that MCPH1, like MDC1, does not recognize this state of H2A.X. At the present time, readers of pTyr142 H2A.X remain undiscovered. Next, we found that with regards to  $\gamma$ H2A.X, MCPH1 and MDC1 can both recognize this state with similar affinities. In the absence of a clear affinity advantage of either MDC1 or MCPH1 for  $\gamma$ H2A.X, their respective levels may determine the amounts recruited. This contention is supported by an earlier study reporting that overexpression of MCPH1 could result in a reduction of MDC1

foci (16). Therefore, overexpressed MCPH1 may outcompete and directly displace  $\gamma$ H2A.X-bound MDC1. It thus appears that tipping the concentration balance in favor of MCPH1 or MDC1 could significantly alter the composition at  $\gamma$ H2A.X nucleosomes. Also, the ability of MDC1 to dimerize in response to DNA damage may considerably change its capacity to bind  $\gamma$ H2A.X with avidity effects coming into play (36, 37). This may explain how MDC1 independently engages  $\gamma$ H2A.X in the presence of MCPH1. Furthermore, both MCPH1 and MDC1 may be present in high molecular weight multicomponent complexes, which could alter the affinities measured using purified recombinant domains. Thus, whereas the BRCT domains of MCPH1 and MDC1 are direct readers of  $\gamma$ H2A.X, this ability may be harnessed as part of larger DNA damage sensing multiprotein assemblies to gain access to sites of DSBs. Such is likely the case for MCPH1, an established component of the BRCA2/Rad51 (33), SWI/SNF (15), and Condensin II (34, 35) complexes that need to be directed to damaged sites. Future work is required to decipher the amounts of MCPH1 parsed into each of these and other complexes and the contribution of MCPH1– $\gamma$ H2A.X interaction toward their targeting.

Whereas considerable strides have been made toward understanding how Ser139-phosphorylated H2A.X controls downstream mediators and effectors, much less is known about H2A.X phosphorylated at both Ser139 and Tyr142. In this study, we have first confirmed the existence of previously hypothesized di- $\gamma$ H2A.X in vivo, a form of H2A.X that exists in the very early phases of DDR. Next, we have shown a clear and unambiguous difference in the ability of two early mediator proteins to engage modified H2A.X. Whereas MDC1 can bind the canonical  $\gamma$ H2A.X state, it shows no affinity toward di- $\gamma$ H2A.X. In contrast, MCPH1 shows the requisite plasticity to sense both the pSer139- and pSer139, pTyr142-modified H2A.X. Our work therefore uncovers the latent ability of a subset of tandem BRCT domains to recognize the pSXXpY motif with important implications for future biology as it provides a distinct recognition strategy for selective recruitment of MCPH1 in early phases of the DDR. The biological significance of the ability of MCPH1 to read both  $\gamma$ H2A.X and di- $\gamma$ H2A.X is yet to be explored. On the basis of the kinetics of  $\gamma$ H2A.X and di- $\gamma$ H2A.X, we speculate that the ability of MCPH1 to bind di- $\gamma$ H2A.X recruits MCPH1 to the damaged sites as one of the earliest responses to DNA damage. As the repair process proceeds, pTyr42 is dephosphorylated, which would allow even stronger interaction between  $\gamma$ H2A.X and MCPH1. This increased affinity could be necessary for the recruitment of other repair factors. If pTyr42 is not dephosphorylated, factors involved in apoptosis might eventually displace MCPH1 to initiate apoptosis, which has previously been suggested to be one of the roles of di- $\gamma$ H2A.X (7, 8). Specifically, our finding forms the basis for selectively inhibiting the MCPH1–H2A.X pathway over the MDC1–H2A.X pathway using di-pH2A.X mimetics. Lastly, our study broadens the scope of tandem BRCT domain recognition sequences, previously restricted to pSer or pThr, to include phosphotyrosine and multiple phosphorylation marks. This discovery speculates that BRCT domains may play a larger role in biological functions than previously anticipated.

## Materials and Methods

Detailed methods for protein production, purification, crystallization, structure determination, ITC measurements, antibody generation, pull-down assays, and immunofluorescence are described in *SI Materials and Methods*. Briefly, MCPH1 and MDC1 were expressed in *Escherichia coli* as N-terminal His<sub>6</sub>-tag fusion constructs and purified by metal affinity and, after cleavage of the His<sub>6</sub>-tag, by size exclusion chromatography. Three dimensional structures of the MCPH1–pH2A.X and MCPH1–di-pH2A.X complexes were determined by molecular replacement from diffraction data recorded at beamline 19-ID of the Advanced Photon Source (APS) at Argonne National Laboratory and beamline X29 of the National Synchrotron Light Source

(NLS) at Brookhaven National Laboratory, respectively. Data collection and refinement statistics are presented in Table 1.

**ACKNOWLEDGMENTS.** We are grateful to Y. Kim at Advanced Photon Source (APS) for assistance with X-ray data collection, Z. Dauter for insightful comments regarding structure refinement, and A. Nussenzweig for providing the *H2a.x<sup>-/-</sup>* mouse embryonic fibroblasts. The MCPH1 construct used for peptide library screening was a kind gift of R. Chahwan and S. P. Jackson, University of Cambridge, Cambridge, United Kingdom. This work was supported by

National Institutes of Health (NIH) Grants CA132878 (to G.M.), CA097134, DK018477, DK39949, and NS034934 (to M.G.R.), CA116167 (to F.J.C.), and CA112967 and ES015339 (to M.B.Y.). M.G.R. is a Howard Hughes Medical Institute investigator. We acknowledge the use of beamline 19-ID at APS and beamline X29 at National Synchrotron Light Source (NLS). APS is operated by University of Chicago's Argonne National Laboratory, for the US Department of Energy under Contract DE-AC02-06CH11357. Funding for NLS comes from the offices of Biological and Environmental Research and Basic Energy Sciences of the US Department of Energy and from NIH Grant P41RR012408.

1. Rogakou EP, Pilch DR, Orr AH, Ivanova VS, Bonner WM (1998) DNA double-stranded breaks induce histone H2AX phosphorylation on serine 139. *J Biol Chem* 273: 5858–5868.
2. Scully R (2010) A histone code for DNA repair. *Nat Rev Mol Cell Biol* 11:164.
3. Stewart GS, Wang B, Bignell CR, Taylor AM, Elledge SJ (2003) MDC1 is a mediator of the mammalian DNA damage checkpoint. *Nature* 421:961–966.
4. Stucki M, et al. (2005) MDC1 directly binds phosphorylated histone H2AX to regulate cellular responses to DNA double-strand breaks. *Cell* 123:1213–1226.
5. Lou Z, et al. (2006) MDC1 maintains genomic stability by participating in the amplification of ATM-dependent DNA damage signals. *Mol Cell* 21:187–200.
6. Xiao A, et al. (2009) WSTF regulates the H2A.X DNA damage response via a novel tyrosine kinase activity. *Nature* 457:57–62.
7. Cook PJ, et al. (2009) Tyrosine dephosphorylation of H2AX modulates apoptosis and survival decisions. *Nature* 458:591–596.
8. Krishnan N, et al. (2009) Dephosphorylation of the C-terminal tyrosyl residue of the DNA damage-related histone H2A.X is mediated by the protein phosphatase eyes absent. *J Biol Chem* 284:16066–16070.
9. Campbell SJ, Edwards RA, Glover JN (2010) Comparison of the structures and peptide binding specificities of the BRCT domains of MDC1 and BRCA1. *Structure* 18:167–176.
10. Jackson AP, et al. (2002) Identification of microcephalin, a protein implicated in determining the size of the human brain. *Am J Hum Genet* 71:136–142.
11. Lin SY, Rai R, Li K, Xu ZX, Elledge SJ (2005) BRIT1/MCPH1 is a DNA damage responsive protein that regulates the Brca1-Chk1 pathway, implicating checkpoint dysfunction in microcephaly. *Proc Natl Acad Sci USA* 102:15105–15109.
12. Rai R, et al. (2006) BRIT1 regulates early DNA damage response, chromosomal integrity, and cancer. *Cancer Cell* 10:145–157.
13. Chaplet M, Rai R, Jackson-Bernitsas D, Li K, Lin SY (2006) BRIT1/MCPH1: A guardian of genome and an enemy of tumors. *Cell Cycle* 5:2579–2583.
14. Bartek J (2006) Microcephalin guards against small brains, genetic instability, and cancer. *Cancer Cell* 10:91–93.
15. Peng G, et al. (2009) BRIT1/MCPH1 links chromatin remodelling to DNA damage response. *Nat Cell Biol* 11:865–872.
16. Wood JL, Singh N, Mer G, Chen J (2007) MCPH1 functions in an H2AX-dependent but MDC1-independent pathway in response to DNA damage. *J Biol Chem* 282: 35416–35423.
17. Jeffers LJ, Coull BJ, Stack SJ, Morrison CG (2008) Distinct BRCT domains in Mcph1/Brit1 mediate ionizing radiation-induced focus formation and centrosomal localization. *Oncogene* 27:139–144.
18. Shao Z, et al. (2012) Specific recognition of phosphorylated tail of H2AX by the tandem BRCT domains of MCPH1 revealed by complex structure. *J Struct Biol* 177: 459–468.
19. Manke IA, Lowery DM, Nguyen A, Yaffe MB (2003) BRCT repeats as phosphopeptide-binding modules involved in protein targeting. *Science* 302:636–639.
20. Yu X, Chini CC, He M, Mer G, Chen J (2003) The BRCT domain is a phospho-protein binding domain. *Science* 302:639–642.
21. Leung CC, Gong Z, Chen J, Glover JN (2011) Molecular basis of BACH1/FANCD1 recognition by TopBP1 in DNA replication checkpoint control. *J Biol Chem* 286:4292–4301.
22. Botuyan MV, et al. (2004) Structural basis of BACH1 phosphopeptide recognition by BRCA1 tandem BRCT domains. *Structure* 12:1137–1146.
23. Shiozaki EN, Gu L, Yan N, Shi Y (2004) Structure of the BRCT repeats of BRCA1 bound to a BACH1 phosphopeptide: Implications for signaling. *Mol Cell* 14:405–412.
24. Williams RS, Lee MS, Hau DD, Glover JN (2004) Structural basis of phosphopeptide recognition by the BRCT domain of BRCA1. *Nat Struct Mol Biol* 11:519–525.
25. Clapperton JA, et al. (2004) Structure and mechanism of BRCA1 BRCT domain recognition of phosphorylated BACH1 with implications for cancer. *Nat Struct Mol Biol* 11:512–518.
26. Kilkenny ML, et al. (2008) Structural and functional analysis of the Crb2-BRCT2 domain reveals distinct roles in checkpoint signaling and DNA damage repair. *Genes Dev* 22:2034–2047.
27. Williams JS, et al. (2010) gammaH2A binds Brc1 to maintain genome integrity during S-phase. *EMBO J* 29:1136–1148.
28. Joughin BA, Tidor B, Yaffe MB (2005) A computational method for the analysis and prediction of protein:phosphopeptide-binding sites. *Protein Sci* 14:131–139.
29. Xu X, Lee J, Stern DF (2004) Microcephalin is a DNA damage response protein involved in regulation of CHK1 and BRCA1. *J Biol Chem* 279:34091–34094.
30. Tibelius A, et al. (2009) Microcephalin and pericentrin regulate mitotic entry via centrosome-associated Chk1. *J Cell Biol* 185:1149–1157.
31. Passemard S, et al. (2011) VIP blockade leads to microcephaly in mice via disruption of Mcph1-Chk1 signaling. *J Clin Invest* 121:3071–3087.
32. Gruber R, et al. (2011) MCPH1 regulates the neuroprogenitor division mode by coupling the centrosomal cycle with mitotic entry through the Chk1-Cdc25 pathway. *Nat Cell Biol* 13:1325–1334.
33. Wu X, et al. (2009) Microcephalin regulates BRCA2 and Rad51-associated DNA double-strand break repair. *Cancer Res* 69:5531–5536.
34. Wood JL, Liang Y, Li K, Chen J (2008) Microcephalin/MCPH1 associates with the Condensin II complex to function in homologous recombination repair. *J Biol Chem* 283:29586–29592.
35. Yamashita D, et al. (2011) MCPH1 regulates chromosome condensation and shaping as a composite modulator of condensin II. *J Cell Biol* 194:841–854.
36. Liu J, et al. (2012) Structural mechanism of the phosphorylation-dependent dimerization of the MDC1 forkhead-associated domain. *Nucleic Acids Res* 40: 3898–3912.
37. Jungmichel S, et al. (2012) The molecular basis of ATM-dependent dimerization of the Mdc1 DNA damage checkpoint mediator. *Nucleic Acids Res* 40:3913–3928.